

Heterogeneous Conforming Compliant Microstructure Mechanisms

Gershon Elber
Computer Science Department
Technion
Haifa 32000, Israel
Email: gershon@cs.technion.ac.il

June 23, 2023

Abstract

The interest in compliant mechanisms is on the rise, in recent years, mostly due to the introduced abilities of additive manufacturing that are able to fabricate highly complex compliant mechanisms, via 3D printing. Yet, so far, the focus in this area has been on the functionality of individual compliant mechanisms.

This work presents a framework to design whole freeform macro-shape microstructure compliant mechanisms, possibly heterogeneous, using compliant mechanism tiles embedded in the macro-shapes. By employing a conforming placement algorithm of compliant mechanism tiles in the macro-shape, a model that serves as a whole compliant microstructure mechanism model can be formed, while preserving the integrity of the individual tiles. Further, different compliant mechanism tiles can be placed in different locations in the microstructure, and as a result, a heterogeneous macro-model compliant microstructure mechanism can be formed, with the desired physical behavior. This work aims to expose and exemplify the potential of this design paradigm, potential that will be demonstrated by several fabricated examples, with the aid of 3D printing.

Keywords: Lattices, Functionally graded material, 3D Auxetic tiles, Bistable tiles, Functional tiles

1 Introduction and Previous Work

The interest in compliant mechanisms [7, 9] has increased, in recent years, mostly due to the introduced abilities of additive manufacturing that enable the fabrication of complex compliant mechanisms, via 3D printing. By *compliant*, it hints to the fact that the mechanism can deform, elastically but not only, under certain physical conditions, typically stress. The fabrication of compliant mechanisms using 3D printing is now simpler than ever, typically having fewer parts, only to fabricate parts with a reduced operational noise as well as diminished wear and tear.

These ideas evolved mostly due to additive manufacturing (AM) technologies that enabled the fabrication with ease, of such structures. In [12], a connection is made between compliant mechanisms and microstructures¹, while the presented examples are all axis-parallel, uniform 3D grid of tiles, in the microstructure. Heterogeneity is somewhat considered via composite/piezoelectric materials. Topological optimization (TO) has also been examined as a solution for compliant macro-shapes behavior. For example, in [20], wings are designed, where geometric nonlinear finite elements are combined with TO to optimize entire wing sections (ribs). In [24, 3], topological optimization has been used to optimize compliant mechanical behavior, including of multi-materials.

Quite a few examples of designs using compliant mechanisms have been published. In [22], compliant spherical flexure joints are designed, similar to traditional ball/socket spherical joints. In [23], bistable tiles are employed toward mechanical logic. The two stable states of a bistable mechanism are exploits to represent '0' and '1' and a careful mechanical design allows for a complete logic set, providing an implementation of AND and NOT (and more) and hence offer a complete sets of binary logic gates. The advantage is that as mechanical devices, they require no power source to hold their logic state. In [2], a multi-state behavior using bistable tiles is achieved by employing

¹in this work, we refer to *microstructures* where others might call lattices - a spatial porous structure, typically as a topological grid.

the bistable tiles as actuators in a serial cascade and even as edges in 3D structures such as tetrahedra. In [10, 15], twisting and turning bistable elements are considered. [15] also demonstrates “reconfigurable surfaces” that can deform from flat shape to 3-space shapes, using carefully placed bistable tiles in (thickened) 2-manifolds.

In computer graphics, typically axis-parallel 3D grid-like microstructures were employed to allow macro-behaviors, such as a deformation of a face under physical pressure [19] or robotic motion and kinematics [8] in the plane. [8] also denotes these structures as metamaterial mechanisms.

Auxetics are special geometries that can demonstrate unnatural behavior, and have been quite heavily investigated, in recent years. With varying Poisson’s ratios², a contraction in one 3D axis, can result in either a contraction or an expansion in another axis or even axes. Auxetics were observed to offer superior properties with respect to shock absorption’s, acoustical isolation, controlled permeability, etc. In [13], a review of those structures, mostly in the plane, but also in 3D axis parallel grid of similar tiles is discussed. In [21], Auxetics structures are reviewed and explored with respect to their geometry and properties. Some applications are proposed such as (medical) stents, protective gears and devices, nails that are easy to hammer in and hard to pull out, and piezoceramic sensors. [11] is another recent review of Auxetic geometries, that also examines manufacturability, applications and mechanical properties of Auxetics.

Planar Auxetics tiles with local adaptation are also employed in shell (thickened 2-manifolds) microstructures. For example, in [14], individual planar Auxetics tiles are locally adjusted in a 2D arrangement, so as to approximate a 3D shell structure, when external forces are applied, such as gravity.

In this work, we show that a next natural step is also feasible - presenting a framework that employs compliant mechanism tiles that are embedded in a general freeform 3-space macro-shape, toward the creation of 3D macro-shape compliant microstructure mechanisms. Given a global 3D macro-shape, \mathcal{M} , a somewhat deformed, possibly heterogeneous (material-wise but also geometrically), incorporated set of compliant mechanism tiles are embedded in \mathcal{M} , while preserving the topological as well as geometrical integrity of individual tiles. All this aimed to achieved some global desirable behavior, over \mathcal{M} .

The rest of this work is organized as follow. In Section 2, we present some necessary background for this work. Then, Section 3 presents several examples, including of 3D printed assemblies, only to conclude and discuss possible future work, in Section 4.

2 Background

The common approach to the creation of microstructures in contemporary commercial CAD system for geometric modeling, is by clipping a 3D uniform grid of similar tiles to the macro-shape \mathcal{M} in hand. See Figure 1 (a). In this work, we are interested in functional micro-tiles, tiles that have certain geometry that is expected to behave or function. Clipping such tiles in an arbitrary way, as is commonly done in contemporary CAD systems, will be devastating to the functionality of those tiles. Further, the clipped tiles are typically on the boundary of \mathcal{M} , a critical region in any (functional) model. In other words, the preservation of the topological and geometrical integrity of individual tiles is crucial when aiming to employ these tiles as compliant mechanisms in a 3D macro-shape compliant microstructure.

Recently, an alternative conforming microstructure reconstruction scheme was proposed in [5, 18]. Using volumetric representations (aka V-reps), based on (trimmed) trivariate splines, they are able to represent interior material properties along with the geometric model, among others. Consider a freeform trivariate macro-shape $\mathcal{M} : D \in \mathbb{R}^3 \rightarrow \mathbb{R}^k$, $k \geq 3$ that is provided as a volumetric trivariate B-spline function. In addition to its 3D geometry, \mathcal{M} is capable of representing scalar, vector, or tensor, etc. properties throughout its encompassed volume, for $k > 3$.

Now consider some geometry $G \in [0, 1]^3$ consisting of univariates (curves) and/or bivariates (surfaces) and/or

²https://en.wikipedia.org/wiki/Poisson's_ratio

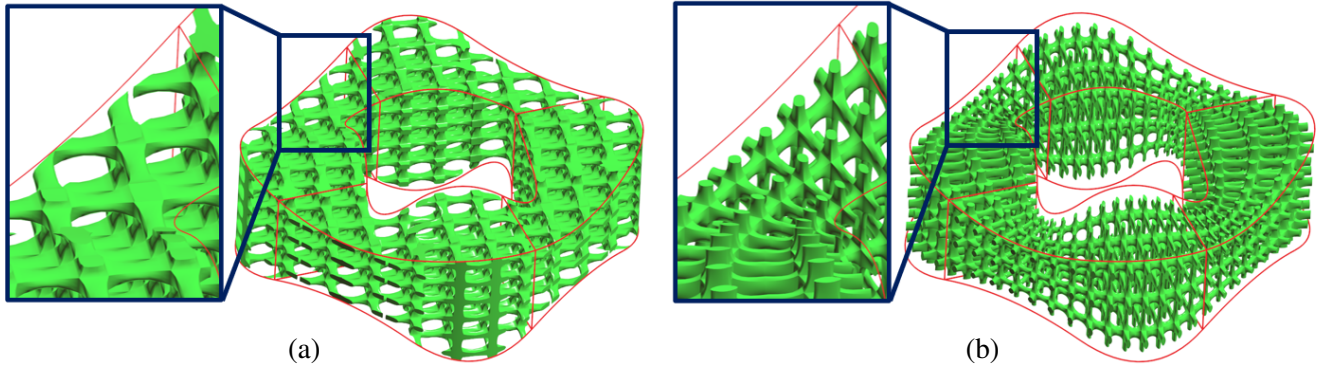


Figure 1: In (a), an axis parallel 3D grid of tiles is being cropped and coerced to be in a torus macro-shape with a square cross section of varying section size. As a result, tiles, especially on the boundary, are being clipped in an arbitrary way. In (b), the tiles follow the 'flow' of the same torus macro-shape, being conforming to it, and no tile is being clipped.

trivariates B-spline function, possibly trimmed. G will be denoted as a *tile* and is typically periodic. That is, boundary $G|_{x=0}$ is identical to boundary $G|_{x=1}$ and same for the Y and Z . In addition, G and its neighbors can optionally be arbitrary smooth on $G|_{x=0}$ and $G|_{x=1}$ and/or the Y and Z boundaries.

Given trivariate \mathcal{M} , G can populate the domain D of \mathcal{M} ($i \times j \times k$) times, only to functionally compose each of the G_{ijk} tiles with \mathcal{M} , as $\mathcal{M}(G_{ijk})$, mapping G_{ijk} to the range of \mathcal{M} . Denote the entire set of tiles $G_{ijk}, \forall i, j, k$, as \mathcal{G} . $\mathcal{M}(\mathcal{G})$ defines a whole microstructure that is conforming to the shape of \mathcal{M} . See Figure 1 (b). Equally important, no tile is being clipped or topologically modified as a result of this functional composition.

As stated, tile G can consist of any set of univariates (curves), bivariates (surfaces), or trivariates (volumetric) B-spline functions. Specifically, by having trivariates in G , one can represent the geometry but also define (graded) heterogeneous tiles. Further, as long as continuity (and smoothness as desired) is preserved between adjacent tiles in D , one can have (parametric) variations of tiles throughout \mathcal{M} . In other words, tiles can differ, in different locations in \mathcal{M} , in their geometry but also in their material content! Figure 2 shows a few heterogeneous trivariate tiles that are employed in this work. These tiles are constructed via a parametric prescription that controls their precise shape (angles, thicknesses, widths, etc.) and material content. This prescription, with varying parameters, can synthesize different variations of the tiles, across and in different locations in \mathcal{M} , and establish the desired (graded) heterogeneity in $\mathcal{M}(\mathcal{G})$.

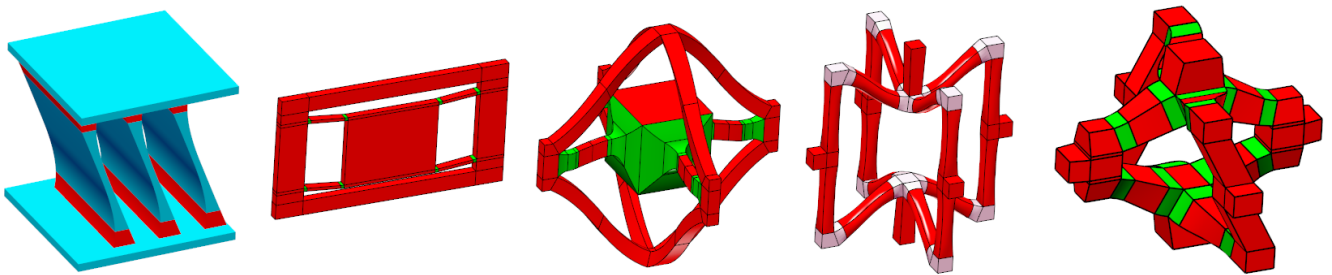


Figure 2: Several heterogeneous trivariate parametric micro-tiles that are employed in this work. Different colors, in each tile, mean different materials.

The fact that the integrity and functionality of individual tiles is preserved in the scheme presented by [5, 18] is, again, crucial to our aim in this work - creating conforming macro-model compliant microstructure mechanisms with (potentially graded) heterogeneity, from individual (compliant) micro-tile mechanisms. In Section 3, we exemplify

this proposed framework, on several cases. For more on the conformal, composition based, lattice construction scheme that the presented framework for compliant microstructure mechanisms is employing, please see [1, 5, 18, 6, 17].

3 Heterogeneous Conforming Compliant Microstructure Mechanisms

We now exemplify the idea of generalizing the concept of compliant mechanisms to freeform heterogeneous compliant microstructure mechanisms. All presented examples, in this work, were 3D printed using the J55 printer of Stratasys³.

As stated, we employ *parametric* tiles in this work, which means the tile's definition can yield specific geometric/material instances out of a continuum n -parameters family of tiles, via a prescribed set of tile's parameters. In other words, a parametric representation defines a continuous family of tiles that can vary in shape and/or material content, based on the prescribed input. This ability is employed, in this entire section, to vary individual tiles in specific location in the macro-shape \mathcal{M} , so as to achieve a desired global (physical) behavior of \mathcal{M} . In this section, we modify the geometry of different tiles at times, but also employ varying hardness materials, in different tiles as well as in different parts of individual tiles. The typical Shore-A hardness of the flexible materials we exploit in this work for hinges is around 50, which is approximately the hardness of a pencil eraser.

The rest of this section is organized as follows. In Section 3.1, a parametric shear tile is employed and demonstrated on different macro-shapes \mathcal{M} . In Section 3.2, a parametric Auxetic tile is exploited, and in Section 3.3, a bistable tile is used.

3.1 Shear tiles

Consider the tiles shown in Figure 3 (a). These tiles consists of rigid materials (in cyan) and flexible materials (in red, with Shore-A hardness of around 50) that serve as hinges. A vertical pressure on such a tile will force it to shear to the side.

In Figure 3, a linear shear microstructure mechanism is designed and presented, by embedding these tiles in a box trivariate macro-shape \mathcal{M} . As can be seen in Figure 3 (b) and (c), each level in this structure is exerting a different amount of shear, by employing a different shear tile, while all tiles are derived from a single parametrically defined tile. Figure 3 (d) and (e) show the 3D printed result while Figures 3 (f₁) to (f₃) are three snapshot from a movie of the mechanism undergoing vertical pressure.

Now, consider a similar shear tile shown in Figure 4 (a), with, again, rigid materials (in cyan) and flexible materials (Shore-A of around 50, in yellow) that serve as hinges. This tile is embedded (many times) in the tube trivariate macro-shape representing \mathcal{M} that is shown in Figure 4 (b). The entire model is shown in Figure 4 (c), with top and bottom covers (in magenta) and five colored wings to better exemplify the expected angular twist. Figure 4 (d) shows the 3D printed model whereas Figure 4 (e₁) shows a view of the model under minimal pressure, and in (e₂) under full pressure. The twists in the colored wings, in (e₃), are due to these shear tiles, under full pressure. In Figure 3, different tiles were used in different levels. Clearly, one can also place different shear tiles at different levels of the rounded tube macro-model \mathcal{M} , in Figure 4 (b), to achieve different desired turning/twisting angles, in different levels.

Interestingly, the model in Figure 4 is related to Kresling pattern origami. While, in general, cylindrical macro-shapes that twist under pressure are considered, in [16] for example, mostly conical shapes are considered with positive, negative, and zero Gaussian curvature. Clearly, one can construct similar microstructures, to the one we present in Figure 4, of different signs of Gaussian curvature, and/or even non circular cross sections, using shear tiles embedded in general trivariate tubes of revolutions.

Figure 5 is our last example using the shear tile. In a similar way to the angular shear in Figure 4, the tiles are placed in a tube-tile macro-shape trivariate, \mathcal{M} . However, in the example presented in Figure 5, the tiles are organized so the shear effect will be radial (outside). Figure 5 (a) shows the entire column of tiles used around \mathcal{M} ,

³<https://www.stratasys.com/en/3d-printers/printer-catalog/polyjet/j55-prime>

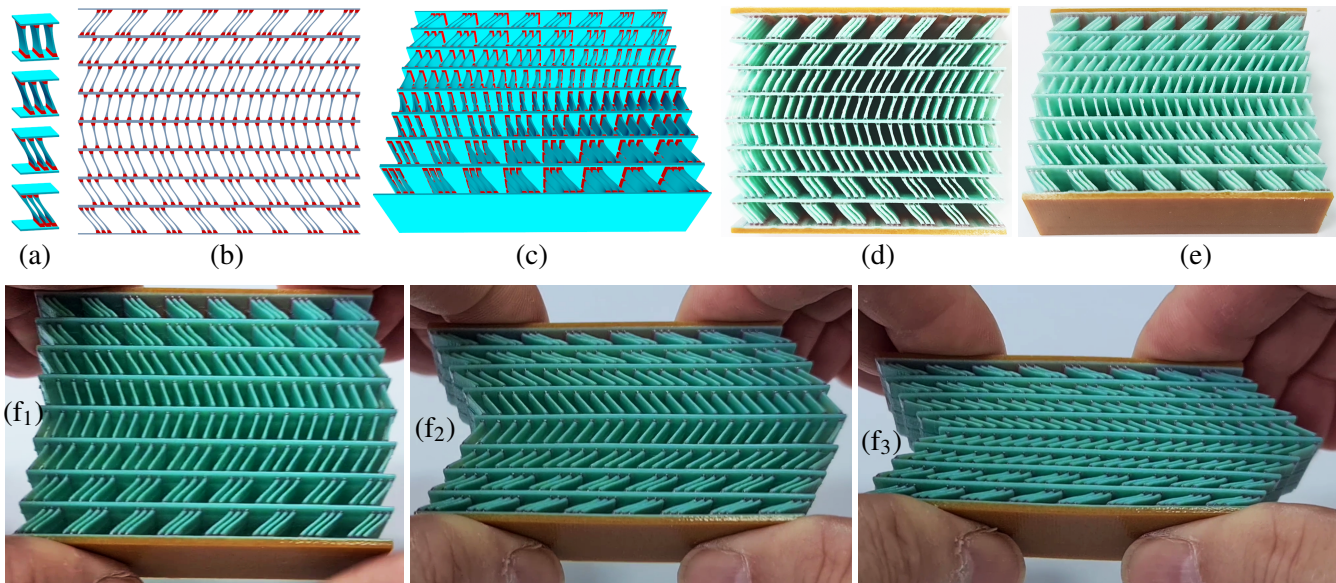


Figure 3: A linear shear compliant microstructure mechanism. In (a), the different shear tiles, that are employed in this model, are presented. (b) and (c) present the 3D final result, $\mathcal{M}(\mathcal{G})$, as a computer model whereas (d) and (e) show the 3D printed counterpart. Finally, (f₁) to (f₃) are three snapshots captured from a movie (<https://youtu.be/gJ4XecdAB4Q>) of this 3D printed model undergoing vertical pressure.

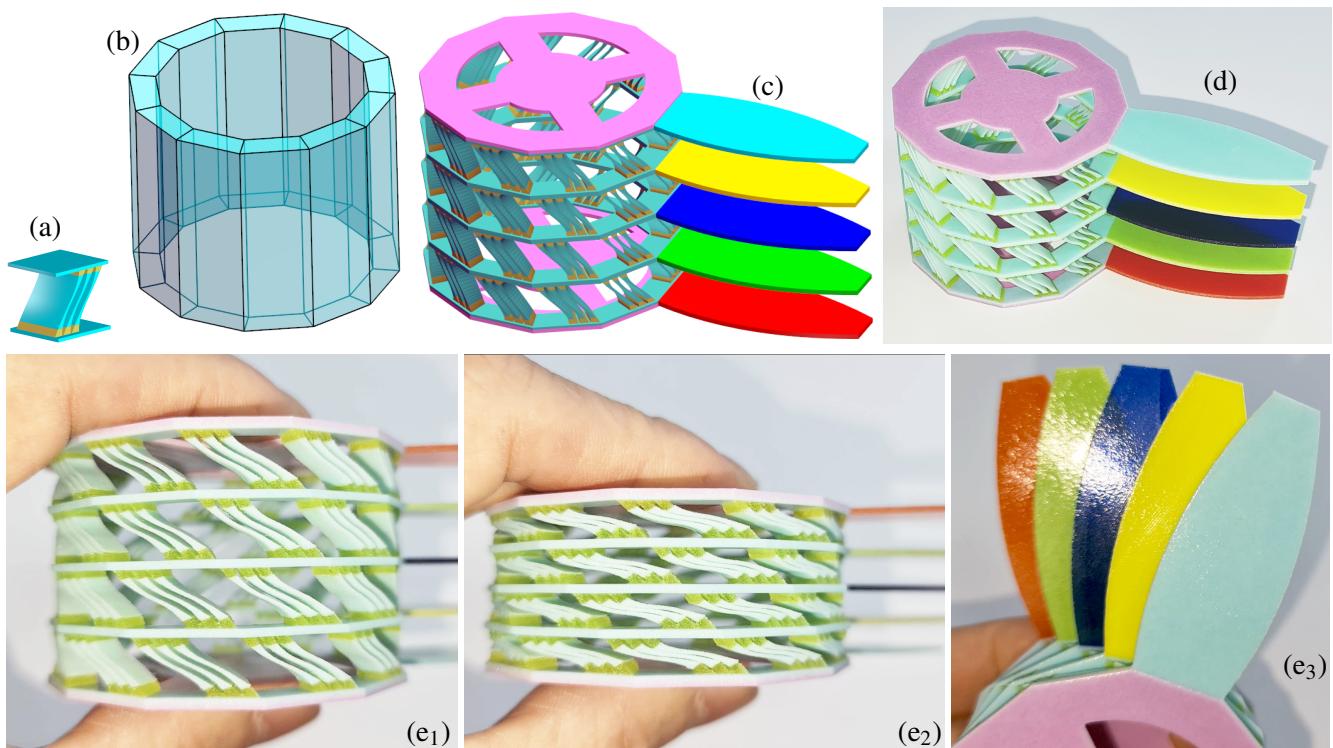


Figure 4: A rounded twisting compliant microstructure mechanism. The shear tile in (a) is populating (many times) the trivariate macro-model \mathcal{M} in (b), via functional composition, and the final model is shown in (c). In (d), the 3D printed model is presented, and (e₁) to (e₃) are snapshots from the short video (<https://youtu.be/c3QUUFxBOyI>), of the mechanism undergoing vertical pressure.

consisting of eight shear tiles, all different. In this variant of the shear tile, two small joints are added, side way, that connect a tile to its immediate neighbors. These two joints are flexible and are intended to preserve the integrity of the entire macro-shape under vertical pressure. Figure 5 (b) shows the computer model whereas Figures 5 (c₁) to (c₃) are three snapshots from a movie of the structure undergoing vertical pressure.

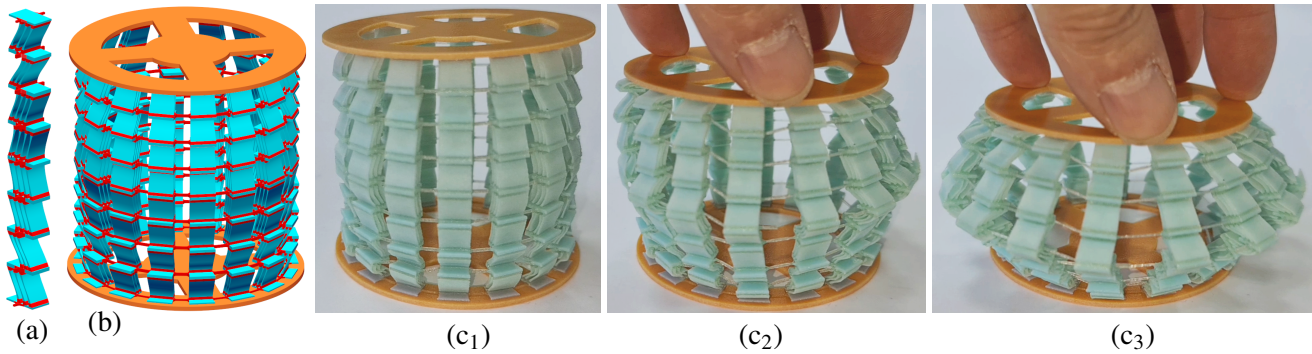


Figure 5: A radial shear compliant microstructure mechanism. The column of eight different shear tiles, in (a), is placed around a cylinder (16 times) to yield (b). (c₁) to (c₃) show the model undergoing vertical pressure, and are from the short video (https://youtu.be/XyXgDm61_Lc). Note This variation of shear tile also employs small joints to its two immediate adjacent tiles, for stability under pressure.

3.2 Auxetic tiles

Figure 6 exemplifies five instances of different parametric heterogeneous Auxetic tiles, of different Poisson's ratios of (left to right): 1.0, 0.5, 0.0, -0.5, -1.0. Herein, the X vs. Z Poisson's ratio and the Y vs. Z Poisson's ratio are all the same, in each tile. The red parts, in Figure 6, are rigid, whereas the light-grey ones are flexible, and serve as hinges. The parameters that control this family of tiles include the Poisson's ratio in $+X -X$, $+Y -Y$ (with respect to Z), that are all independent and can all be different, whether the bars should be rounded or with a square cross section, the thicknesses of the bars and the sizes of the hinges, and optional joints to neighboring tiles/boundary, etc.

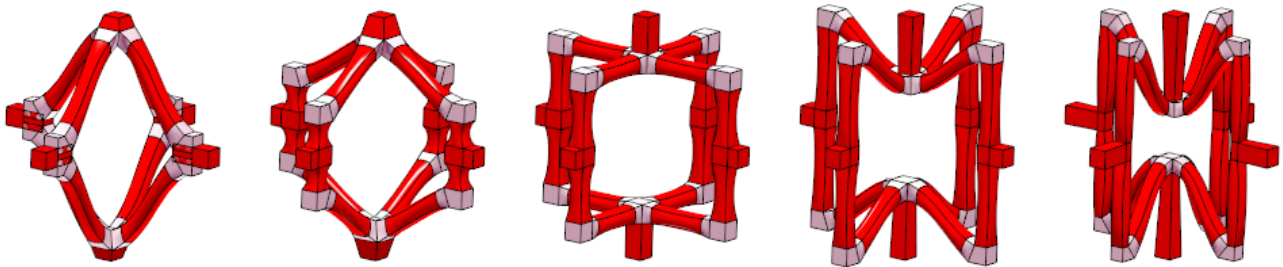


Figure 6: Several samples of different parametric Auxetic tiles that are heterogeneous, with rigid (in red) and flexible (in light-grey) materials.

Consider the barrel macro-shape trivariate in Figure 7 (a) that we seek to populate with Auxetic tiles, from the family of tiles presented in Figure 6. This barrel is populated with different Auxetic tiles in different locations so as to result with the lifting of the two wings, under vertical pressure, wings that are shown in the full computer model, in Figure 7 (b) and (c). All parts in this full model are rigid except the light-grey joints in the Auxetic tiles.

Figures 7 (d₁) to (d₃) show three instances from a movie where a vertical pressure is applied to this model. Specifically, observe the deformations that the central tiles undergo, in Figures 7 (d₁) and (d₂), that are marked by the green rectangles. The two tiles, in the marked rectangle in Figure 7 (d₁), with negative Poisson's ratio at the top and positive Poisson's ratio at the bottom, behave differently, as expected under vertical force - the top tile shrinks horizontally whereas the bottom tile expands horizontally. Compare these two tiles in Figure 7 (d₁) with the same

tiles in Figure 7 (d₂) while under some pressure.

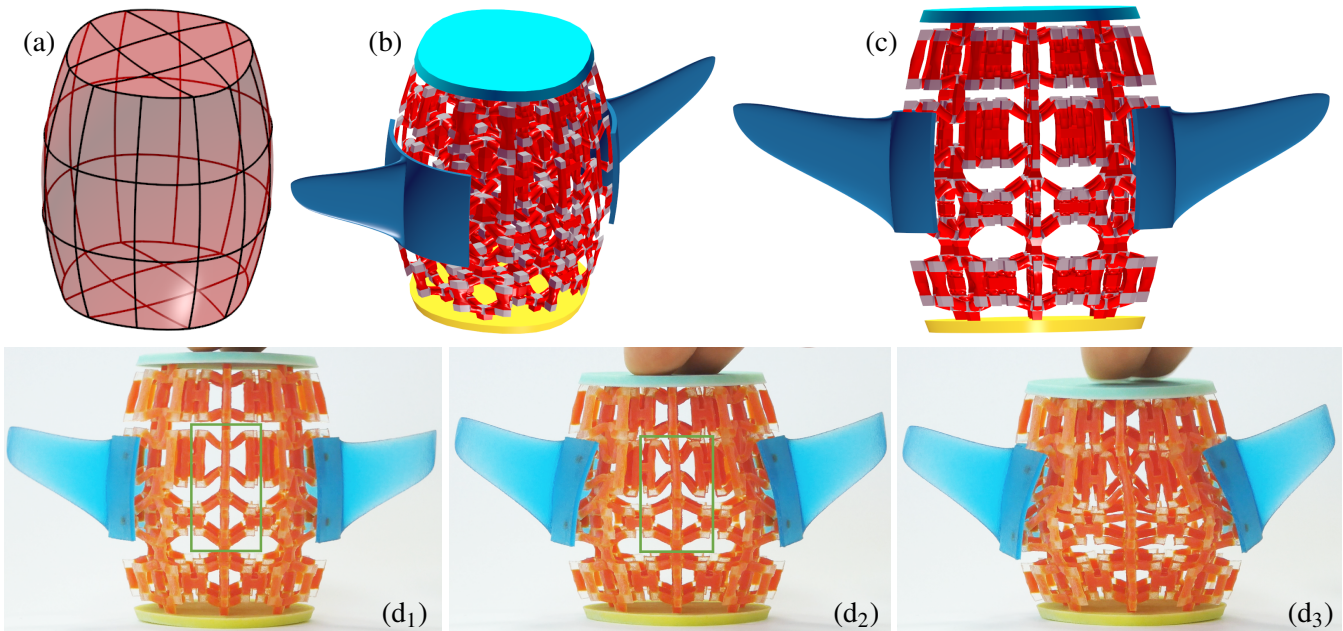


Figure 7: An Auxetic based compliant microstructure mechanism, in a 3D barrel shape (a). Tiles from the family of tiles in Figure 6 are functionally composed into this barrel macro-shape trivariate \mathcal{M} that is shown in (a). The full computer model with a base, top, and side wings is shown in (c) and (d). Then (f₁) to (f₃) are snapshots from a movie (<https://youtu.be/NKck4N7TKQI>) captured of this 3D printed model undergoing vertical pressure.

In Figure 8, we employ tiles from the same family of Auxetic tiles shown in Figure 6 while, this time, square cross sections are used for the tile's arms and each of the tiles possess different Poisson's ratios in X and Y . Again, the red arms of the tiles are rigid, whereas the light-grey ones are flexible, and serve as hinges. The full computer model of a ring of different Auxetic tiles is shown in Figure 8 (a) from a general view from from above, in (c). (b) presented the 3D printed model, for the same view as in (a). The above views of (c) and (d₁) show that the tiles are organized so they form two perfect circles - interior and exterior. Yet, once pressure is applied from above (to the cyan ring), the perfect circularity is broken as can be seen in Figures 8 (d₂) and (d₃) of the 3D printed model.

Our last Auxetic example is presented in Figure 9. In Figure 9 (a), we employ a tile that exerts a negative Poisson's ratio in X (vs. Z) while exerting a positive Poisson's ratio in Y (vs. Z). The same tile is employed throughout the macro-model in the shape of a cylinder, as seen in Figures 9 (b) to (d). In Figure 9 (b), the, mostly, negative Poisson's ratio side is shown from an XZ view, whereas in Figure 9 (c), the, mostly, positive Poisson's ratio side is presented from a YZ view. Then, Figure 9 (d) shows a general view of the model, as well as a zoom-in on one highlighted tile. A vertical pressure on this model, will result with shrinkage in the middle of the model in X while in Y , it will expand.

In Figure 9 (e), a variant of the tile in Figure 9 (a) is shown, a variant that aims to overcome a difficulty in having bars of adjacent tiles vertically colliding, once pressure is applied to the structure (and it shrinks vertically). Figure 9 (f) shows a view of the macro-model cylinder that employs this tile from (e) and in Figures 9 (g) and (h), the structure is shown from the two principal directions, while under vertical pressure.

3.3 Bistable tiles

In Figure 10, we exemplify the use of 2D (with some thickness) bistable tiles. These tiles, as hinted by their name, have two stable states. For instance, on an impact of a certain magnitude, they can switch their state. Rods at some

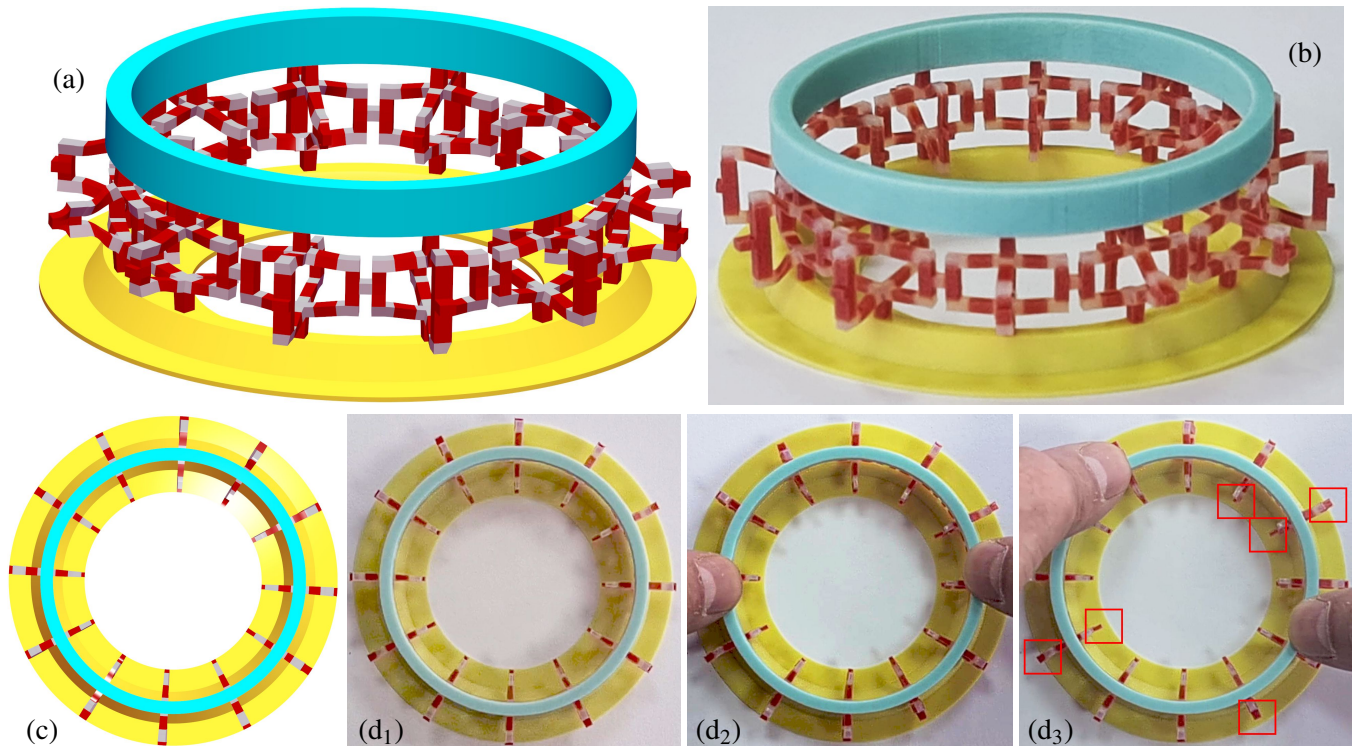


Figure 8: An Auxetic based compliant microstructure mechanism, in a ring. Tiles from the family of tiles in Figure 6 are functionally composed into a square cross section ring macro-shape trivariate. The full computer model with a base (in yellow) and top pressing ring (in cyan) is shown in (a). (b) presents the 3D printed version. (c) and (d₁) show a top view of the computer model and the 3D printed version. Then, (d₂) and (d₃) are snapshots while pressing down the cyan pressing ring. Note the horizontally moving parts, marked using red rectangles, in (d₃), compared to (d₁).

small angle are connected to a central weight, and with a large enough impact, the weight will shift to a reciprocal state.

Figure 10 (a) portrays different samples of 2D bistable heterogeneous parametric tiles. The tiles have rods, that vary in their thicknesses as well as having different angles, that connect to the central weight. The connecting rods have three parts: the central being rigid (in red) and the two end parts are flexible (in green), serving as hinges. Other available parameters in these tiles include the (length) ratios of flexible and rigid regions in the connecting rods, the dimensions of the central weight as well as the entire frame, dimensions in the plane but also in Z , etc.

Figure 10 (b) shows a 4-sided trivariate disk macro-shape, \mathcal{M} , that the 2D bistable tiles are functionally composed with. In this specific design, and due to the nature of this tile, the aim was to preserve parallelism in the tiles while they are mapped through \mathcal{M} . Hence, tiles were mapped only in the angle preserving (conformal) regions of \mathcal{M} . The resulting functionally composed structure is shown in Figure 10 (c) as a computer model and in (d) as the 3D printed heterogeneous model, albeit in different colors.

Figures 10 (e) and (f) show zoom-ins over one column of bistable tiles in this structure, in the two possible states of these tiles. Then, Figures 10 (g) and (h) show different designs with placements around a disk. The placement in (g) has more columns of tiles around the disk while the placement in (h) is no longer conformal and also is presenting geometries of individual parts in the tiles that are different, like the thicker and heavier weights, all created with similar ease via the parametric tile's definition. Also note that the macro-shape, \mathcal{M} , in Figure 10 (h), allows for the placement of tiles in a more condensed fashion, yet, again, at the cost of no conformality in the mapping of the individual tiles. The computer models in Figure 10 present the rigid material in red and the flexible material is

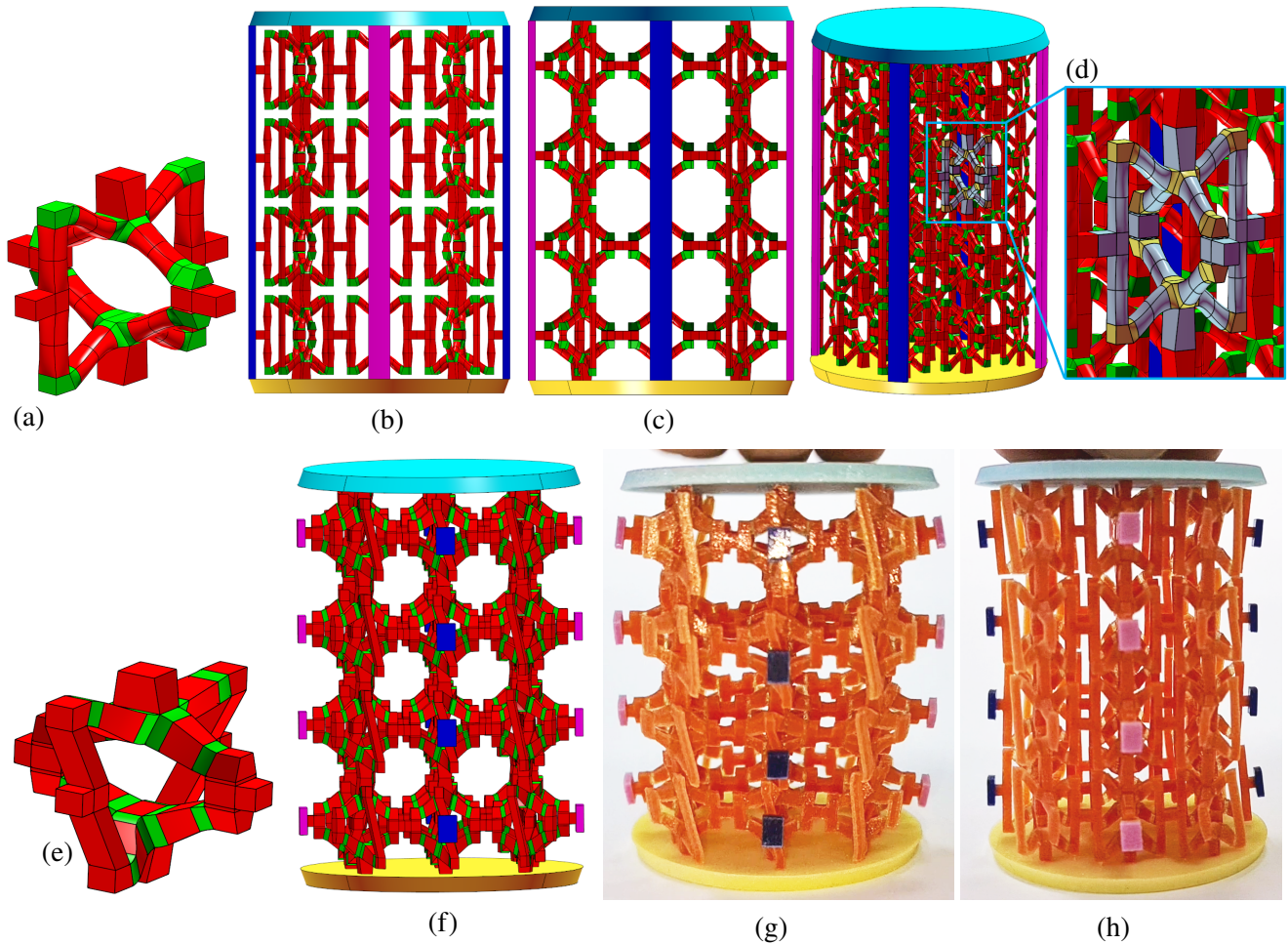


Figure 9: An Auxetic cylinder with different Poisson's ratio in X and Y . (a) shows the basic Auxetic tile while (b) to (d) show a microstructure with a cylinder macro-model and the tile from (a) from the XZ view, the YZ view, and a general view, respectively. (d) also shows a zoomed-in on a single tile, highlighted in cyan. (e) presents a variation of the tile in (a) that aims to eliminate the potential collisions, in Z , between adjacent tiles, that undergo large vertical pressure and significant deformation. (f) shows the entire macro-model, using the tile in (e), whereas (g) and (h) show the 3D printed model in two principal orthogonal views, and under vertical pressure - horizontally expanded (in (g)) and horizontally contracted (in (h)).

shown in green.

Finally, in Figures 10 (i) and (j), we explore the option of having full 3D bistable mechanisms as tiles in a 3D microstructure compliant mechanism. Figure 10 (i) shows three instances of a parametric 3D bistable mechanisms with connecting rods of varying complexity. Then, Figure 10 (j) shows one example of a full 3D placement of these 3D tiles, embedded in a sphere, again, via functional composition.

By incorporating bistable tiles in different orientations as well as with different impact responses, in different rings in the, flat 2D, macro-shape, \mathcal{M} , one can measure different impacts of different magnitudes, from different directions in one plane. This, using a 2D placement of tiles in a disk arrangement. Further, we can even support impact responses of different magnitudes from a full set of 3D directions via a full 3D tile arrangement inside a trivariate macro-shape sphere.

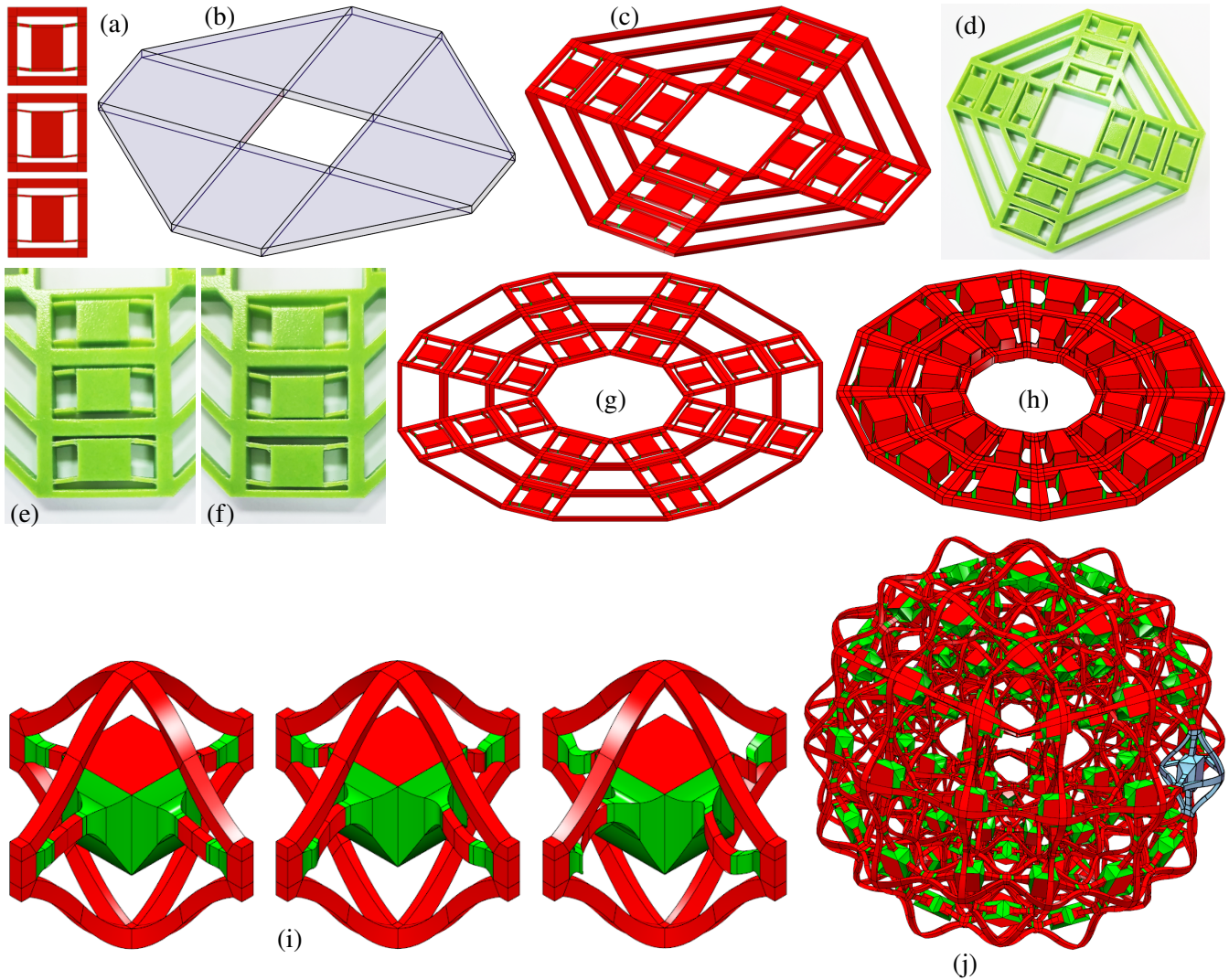


Figure 10: *Bistable based compliant microstructure mechanisms. Examples of bistable tiles are shown in (a) for 2D tiles and in (i) for 3D tiles. With the trivariate macro-shape in (b) and tiles as in (a), (c) can be formed using functional composition and is also shown in (d) after 3D printing, albeit in different colors. (e) and (f) zoom-in on one column of this structure, in its two stable states, whereas (g) and (h) show other parametric design possibilities in 2D. Finally, (j) shows a 3D spherical example using tiles from (i) and a spherical V-rep micro-shape, with one tile highlighted in cyan. See also the video in <https://youtu.be/bag1A1XZ3Dw> that shows a 2D printed disk, populated with bistable tiles, undergoing some impact and flipping a bistable state. All presented computer geometry is in red for rigid parts and in green for the flexible hinges.*

Bistable based microstructure mechanisms can also be used as collapsible structures or “configurable 3D structure”, as they are denoted in [15] (for surfaces). That is, by exploiting the two stable states of the bistable tile, 3D macro-shapes can be formed that can assume two extreme stable states: either a fully open state or fully closed (collapsed) state. In Figure 11, such a structure is presented. Figure 11 (a) shows the bistable tile formed out of both rigid (in magenta) and flexible (in yellow) materials. Then, the green trivariate macro-shape \mathcal{M} of a conical tube that is part of a cup, in Figure 11 (b), is populated with this tile and the functional composition result is shown in Figure 11 (c). Figure 11 (d) shows the model as it was 3D printed, in its expanded stable state, whereas Figure 11 (e)

shows the same model stable, but collapsed.

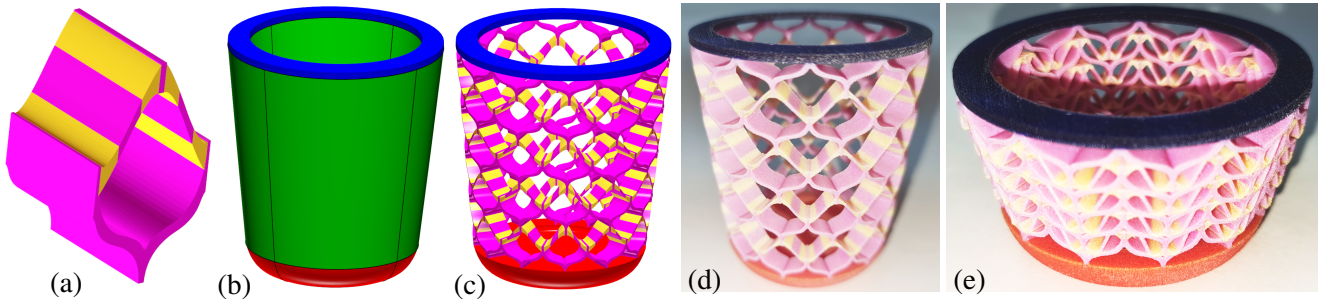


Figure 11: *Bistable based compliant collapsing microstructure mechanism. The employed bistable tile is shown in (a), with both rigid (in magenta) and flexible (in yellow) materials. (b) shows the macro-shape model where the green middle conical tube is populated with the tile from (a), resulting in (c), using functional composition. Finally, (d) and (e) show the 3D printed part. (d) shows the fully expanded stable state (as it was 3D printed) and (e) shows the fully collapsed stable state, from a short video in <https://youtu.be/BxLATHdefRs> that presents the collapsing and expansion steps of this 3D printed cup.*

All the presented examples in this section were represented in a volumetric representation (V-rep) of heterogeneous B-spline trivariates (with material information) that is fully compatible with iso-geometric analysis (IGA) [4]. The adjacent trivariates are IGA's boundary-conforming, which means no mortar methods are required, in the analysis of these structures, in common faces of adjacent trivariates. These examples can also be directly mapped with ease, into classic (heterogeneous) hexa (cuboid) finite elements, and at any desired resolution. Finally, all these examples were synthesized on a modern PC workstation, in a fraction of a second to a few seconds.

4 Conclusions and Future Work

In this work, we have presented a framework to manage compliant microstructure mechanisms. The individual tiles can be heterogeneous, they are never clipped and are positioned, using functional composition, in a conforming way, in the input macro-shape, \mathcal{M} . While in many of the presented examples, we chose simple geometries, like cylinders and rings, nothing in the presented framework prevents one from using general, freeform geometries.

The presented macro-shape structures in Figures 7 and 9 works reasonably well under small forces. Yet, these Auxetic tiles buckle under larger forces. To enable similar uses under large deformations, some stabilizing geometry must be employed to ensure the orientation of individual tiles is preserved, under pressure.

The employed tiles were carefully designed for the different tasks but manually so. Clearly, with the aid of analysis and (topological) optimization tools, e.g. [24, 3], one could hope to achieve more efficient, stable, superior, and optimal tiles, for the different tasks. No claim should be made that the presented tiles are optimal in any way, in our demonstrated tasks. For example, the geometries of the tiles presented in Figures 6 and 10 (a) have been exemplified in many previous work results. Yet, and while intuitive and common, no optimality claims (under some physical conditions) were made on those structures, to the best of our knowledge.

The tiles, in most presented examples in this work, underwent some (non linear) deformation due to the functional composition with the trivariate that represents \mathcal{M} . While these deformations are typically minor, in the local, they are likely to affect the physical properties of the tiles, to a certain extent. High fidelity analysis should be employed to verify and further optimize these structures. Then, the placements of tiles in general orientations that achieve a certain functional behavior or follow a desired direction might be advantageous at times, an extension that should be explored as well.

In [23], bistable tiles were used to mechanically represent logic gates. Extending the framework presented herein to also handle mechanical logic gates in 2D, but also in 3D, is a clear viable directions. Same goes for the

result presented in Figure 11 where the bistable tiles were used as a shell structure - such collapsing structures could also be designed and employed in full 3D. Along similar lines, while herein we have used bistable tiles to construct bistable macro-shape microstructures, one should also consider the creation of multi-stable microstructures using bistable tiles. In every specific macro-shape state, only a partial set of bistable tiles will flip state.

This work presented a framework for heterogeneous compliant microstructure mechanisms. It is our hope that this framework will be found useful for many other heterogeneous compliant microstructure mechanisms, and in different applications. We have demonstrated three types of tiles: shear, Auxetic, and bistable tiles. Yet, clearly many other types of tiles could and should also be considered, for example, toward the design and support of more complex, general, motion. Further, while we did demonstrate the ability to position tiles that are different geometrically as well as with different material content in \mathcal{M} , tiles with different topologies could also be employed in one macro-shape. For instance and given the right application, one can consider having bistable tiles and Auxetic tiles in the same macro-shape. This, while preserving the continuity (as well as smoothness) between adjacent tiles.

Due to our own 3D printing abilities, our focused designs were on responses to forces or pressures. Yet, one could equally envision similar compliant microstructure designs that respond to arbitrary physical stimulus, let it be moisture, light, temperature, electromagnetic radiation, etc. Additive manufacturing stands on three pillars: hardware, software, and materials. Clearly, the pillar of materials is a key to supporting all these different physical stimuli designs.

5 Acknowledgments

This project has received funding from the European Union Horizon 2020 research and innovation programme, under grant agreement No 862025

References

- [1] ANTOLIN, P., BUFFA, A., COHEN, E., DANNENHOFFER, J. F., ELBER, G., ELGETI, S., HAIMES, R., AND RIESENFELD, R. Optimizing micro-tiles in micro-structures as a design paradigm. *Computer-Aided Design 115* (2019), 23–33.
- [2] CHEN, T., MUELLER, J., AND SHEA, K. Integrated design and simulation of tunable, multi-state structures fabricated monolithically with multi-material 3d printing. *Scientific Reports 7*, 45671 (2017), 1–8.
- [3] CHU, S., GAO, L., XIAO, M., LUO, Z., AND LI, H. Stress-based multi-material topology optimization of compliant mechanisms. *Int J Numer Methods Eng.* (2018).
- [4] COTTRELL, J. A., HUGHES, T. J., AND BAZILEVS, Y. *Isogeometric analysis: toward integration of CAD and FEA*. John Wiley & Sons, 2009.
- [5] ELBER, G. Precise construction of micro-structures and porous geometry via functional composition. In *International conference on mathematical methods for curves and surfaces* (2016), Springer, pp. 108–125.
- [6] HONG, Q. Y., AND ELBER, G. Conformal microstructure synthesis in trimmed trivariate based v-reps. *Computer-Aided Design 140* (2021), 103085.
- [7] HOWELL, L. L. *Compliant Mechanisms*. Wiley, 2001.
- [8] ION, A., LINDLBAUER, D., HERHOLZ, P., ALEXA, M., AND BAUDISCH, P. Understanding metamaterial mechanisms. In *Proceedings of the 2019 CHI Conference on Human Factors in Computing Systems* (New York, NY, USA, 2019), CHI '19, Association for Computing Machinery, pp. 1–14.
- [9] JAGTAP, S. P., DESHMUKH, B. B., AND PARDESHI, S. Applications of compliant mechanism in today's world - a review. In *Journal of Physics: Conference Series, IRMAS 2021* (2021).
- [10] JEONG, H. Y., AN, S.-C., SEO, I. C., LEE, E., HA, S., KIM, N., AND JUN, Y. C. 3d printing of twisting and rotational bistable structures with tuning elements. *Scientific Reports 9*, 324 (2019).

- [11] JIANG, W., REN, X., WANG, S. L., ZHANG, X. G., ZHANG, X. Y., LUO, C., XIE, Y. M., SCARPA, F., ALDERSON, A., AND EVANS, K. E. Manufacturing, characteristics and applications of auxetic foams: A state-of-the-art review. *Composites Part B: Engineering* 235 (2022), 109733.
- [12] KIKUCHI, N., NISHIWAKI, S., FONSECA, J. S. O., AND SILVA, E. C. N. Design optimization method for compliant mechanisms and material microstructure. *Comput. Methods Appl. Mech. Engrg.* 151 (1998), 401–417.
- [13] KOLKEN, H. A., AND ZADPOOR, A. A. Auxetic mechanical metamaterials. *RSC Adv.* 7 (2017), 5111–5129.
- [14] KONAKOVIĆ-LUKOVIĆ, M., PANETTA, J., CRANE, K., AND PAULY, M. Rapid deployment of curved surfaces via programmable auxetics. *ACM Trans. Graph.* 37, 4 (jul 2018).
- [15] LI, Y., CHANDRA, A., DORN, C. J., AND LANG, R. J. Reconfigurable surfaces employing linear-rotational and bistable-translational (lrbt) joints. *International Journal of Solids and Structures* 207 (2020), 22–41.
- [16] LU, L., DANG, X., FENG, F., LV, P., AND DUAN, H. Conical kresling origami and its applications to curvature and energy programming. *Proc. Royal Society A.* 478: 20210712. 20210712. (2021).
- [17] MASSARWI, F., AND ELBER, G. A b-spline based framework for volumetric object modeling. *Computer-Aided Design* 78 (2016), 36–47. SPM 2016.
- [18] MASSARWI, F., MACHCHHAR, J., ANTOLIN, P., AND ELBER, G. Hierarchical, random and bifurcation tiling with heterogeneity in micro-structures construction via functional composition. *Computer-Aided Design* 102 (2018), 148–159.
- [19] PANETTA, J., ZHOU, Q., MALOMO, L., PIETRONI, N., CIGNONI, P., AND ZORIN, D. Elastic textures for additive fabrication. *ACM Trans. Graph.* 34, 4 (jul 2015).
- [20] REINISCH, J. Synthesis of compliant mechanisms for morphing wings with nonlinear topology optimization. Master's thesis, TU Munich, 2018.
- [21] REN, X., DAS, R., TRAN, P., NGO, T. D., AND XIE, Y. M. Auxetic metamaterials and structures: a review. *Smart Materials and Structures* 27, 2 (jan 2018), 023001.
- [22] ROMMERS, J., VAN DER WIJK, V., AND HERDER, J. L. A new type of spherical flexure joint based on tetrahedron elements. *Precision Engineering* 71 (2021), 130–140.
- [23] SONG, Y., PANAS, R. M., AND CHIZARI, S. Additively manufacturable micro-mechanical logic gates. *Nature Communication* 10 (2019), 1–6.
- [24] XIA, Q., AND SHI, T. Topology optimization of compliant mechanism and its support through a level set method. *Computer Methods in Applied Mechanics and Engineering* 305 (2016), 359–375.